

THE BIPOLAR MOLECULAR OUTFLOW OF V645 CYGNI¹

A. SCHULZ

Max-Planck-Institut für Radioastronomie, Bonn

J. H. BLACK, C. J. LADA, AND B. L. ULICH

Steward Observatory, University of Arizona

R. N. MARTIN

IRAM, Grenoble; and Steward Observatory, University of Arizona

AND

R. L. SNELL AND N. J. ERICKSON

Five College Radio Astronomy Observatory, University of Massachusetts, Amherst

Received 1988 April 8; accepted 1988 November 1

ABSTRACT

We present a map of the CO $J = 3-2$ line emission from the cloud associated with V645 Cygni. Line wings extending to 15 km s^{-1} on either side of the central velocity can be attributed to a bipolar outflow over a region $1'$ in angular extent. The redshifted and blueshifted emission peaks are separated by $20''$ along an axis that is approximately perpendicular to the polarization vector of the visible light. The outflow is of relatively low velocity, low mass, and low mechanical luminosity.

Subject headings: interstellar: molecules — stars: formation — stars: individual (V 645 Cyg) — stars: mass loss — stars: winds

I. INTRODUCTION

The visible object V645 Cyg was first classified by Hoffmeister, Rohlfs, and Ahnert (1951) as a variable star of long period and was subsequently found to coincide in position with the infrared source AFGL 2789 (Price and Walker 1976; Joyce *et al.* 1977). Detailed optical studies of the object were carried out by Cohen (1977) and by Humphreys, Merrill, and Black (1980). The visible image shows a starlike knot (N0) and a few filamentary nebulosities, the brightest of which is called N1. The visible spectrum is characteristic of a Herbig Ae star, with displaced absorption at velocities up to -340 km s^{-1} (LSR) and strong emission lines, some of which show P Cygni-type profiles. This spectrum does not, however, reveal directly the nature of the underlying star. Infrared studies (Humphreys, Merrill, and Black 1980; Harvey and Lada 1980) show an energy distribution that rises steeply longward of $1 \mu\text{m}$ wavelength and a spectrum with H I Brackett emission lines and the 10 and $20 \mu\text{m}$ absorption features of silicates. Fluxes from Harvey and Wilking (1982) and from the *IRAS Point Source Catalog* (1984) indicate that the energy per decade is nearly constant between $5 \mu\text{m}$ and $100 \mu\text{m}$. VLBI observations show that the H_2O maser emission at $V_{\text{LSR}} = -48 \text{ km s}^{-1}$ arises exactly from the position N0 (Lada *et al.* 1981). Unusual OH maser emission has also been reported, and one possible explanation of it is in terms of a rotating disk (Morris and Kazes 1982). Aside from the marginal fluxes reported by Cohen (1977), only upper limits exist on the radio continuum emission at 5 and 15 GHz (Kwok 1981). The $J = 1-0$ line emission of CO reveals a cloud at $V_{\text{LSR}} = -44 \text{ km s}^{-1}$ apparently associated with V645 Cyg (Harvey and Lada 1980; Rodríguez, Torrelles, and Moran 1981) and shows some evidence of high-velocity line wings. At higher angular resolution, the CO $J = 2-1$ line also exhibits characteristics of a bipolar outflow

(Torrelles *et al.* 1987). The distance of V645 Cyg, the nature of the underlying star, and the physical conditions in its environment have remained controversial.

The aim of the present work was to investigate the distribution and kinematics of the molecular gas in the $J = 3-2$ transition of CO, which affords a probe at higher angular resolution of the gas closest to the central source.

II. OBSERVATIONS

Observations of V645 Cyg were carried out at the frequency of the CO $J = 3-2$ line, 345.796 GHz, during the period 1984 April 17–24 at the Multiple Mirror Telescope Observatory on Mount Hopkins, Arizona (altitude 2600 m). The six 1.83 m mirrors of the Multiple Mirror Telescope were used as a phased submillimeter array with an angular resolution at this frequency equivalent to that of a 7 m telescope. A submillimeter beam combiner placed in front of the normal optical beam combiner brought the six beams to a common focus. The receiver was the cooled 345 GHz Schottky diode mixer of the University of Massachusetts coupled with a 256 channel filter spectrometer of the Max-Planck-Institut für Radioastronomie. The 1 MHz filter width corresponds to a velocity resolution of 0.87 km s^{-1} . The receiver system noise temperature was typically 1200 K, and the scaling system temperature, including contributions from the telescope and atmosphere, was 2700–6000 K (dependent on elevation), with a typical value of 3500 K. Calibration was done by comparison with an ambient load that was assumed to have the same temperature as the sky. Because the attenuating layer of water vapor is close to the ground, this assumption will not cause serious errors. Atmospheric optical depths at zenith ranged from 0.1 to 0.5 for the measurements reported here.

The alignment of each of the individual beams was optimized by measurement of a cold (liquid nitrogen temperature) load in front of the secondary mirrors. The six beams were phased together by using the total power signal of a small

¹ Observations reported here were obtained at the Multiple Mirror Telescope Observatory, a joint facility of the Smithsonian Institution and the University of Arizona.

source, Jupiter, whose angular size is of the same order as that of the synthesized beam. The phasing was checked during each night and was found to remain constant over each observing period. The response pattern of the combined beam consists of a circular main lobe containing 23% of the power and substantial side lobes located $45''$ – $80''$ from the center of the main lobe. Hence, only for sources of $\leq 1'$ size one can expect to be free of considerable beam smearing effects. The full width at half-maximum (FWHM) of the main lobe was measured to be $26''$. The orientation of the radio beam with respect to the optical beam was established to an absolute accuracy of $\pm 10''$ by observing Jupiter and Saturn. Relative positional accuracy within the map presented here is better than $3''$. Owing to the complicated beam pattern, the beam efficiency depends upon source structure: in the present context, the corrected beam efficiency is approximately 0.8 for the extended ($3'$ – $4'$ scale) emission at velocities near the line core, and is approximately 0.33 for the high-velocity emission that is localized within about $1'$ diameter.

Because both the submillimeter receiver and the echelle spectrograph could remain mounted on the telescope at the same time, a changeover between optical and submillimeter observing could be made in a matter of minutes. This permitted an experiment in flexible telescope scheduling in which the selection between optical and submillimeter observing programs each night would be based upon a measurement of precipitable water vapor in the atmosphere during the afternoon. As a result, the submillimeter experiment could take advantage of the best conditions of atmospheric transparency while minimizing the waste of inferior periods that were still perfectly acceptable for high-resolution optical spectroscopy.

The CO spectra were measured in a position-switching mode with alternating 60 s on-source integrations and integrations of equal duration at a reference position offset $-15'$ in azimuth. The total integration time per spectrum was usually 10 minutes, and the final data set consists of at least two such spectra per position (five spectra at the center). The antenna temperatures T_A^* reported here have been corrected for losses in the atmosphere and telescope and are estimated to be accurate to $\pm 10\%$. As discussed above, different beam efficiencies have been applied to the extended and localized components of the emission.

III. RESULTS

The map of CO $J = 3-2$ line emission comprised 25 points with a spacing of $20''$ and was centered on the position of the visible object at $\alpha = 21^{\text{h}}38^{\text{m}}10^{\text{s}}.6$ and $\delta = +50^{\circ}00'43''$ (epoch 1950.0). Figure 1 shows three typical spectra at the central position and two offset positions that illustrate the variation in profile structure.

Figure 2 (Plate 8) shows the map integrated line emission for the line core (i.e., integrated over the velocity range of -48.0 to -40.4 km s^{-1} , LSR) superposed on the visible image published by Cohen (1977). Table 1 summarizes the values of peak temperature, central velocity, and line width for the core component together with the corresponding values for the $J = 1-0$ and $J = 2-1$ transitions taken from the literature. For the $J = 1-0$ line, the blending of core and wing components is so severe that only an upper limit on line width can be estimated (Rodríguez, Torrelles, and Moran 1981; Bally and Lada 1983). These data indicate an increase in core line width with increasing rotational quantum number of the upper state, J' . There is evidently no velocity gradient in the extended line core

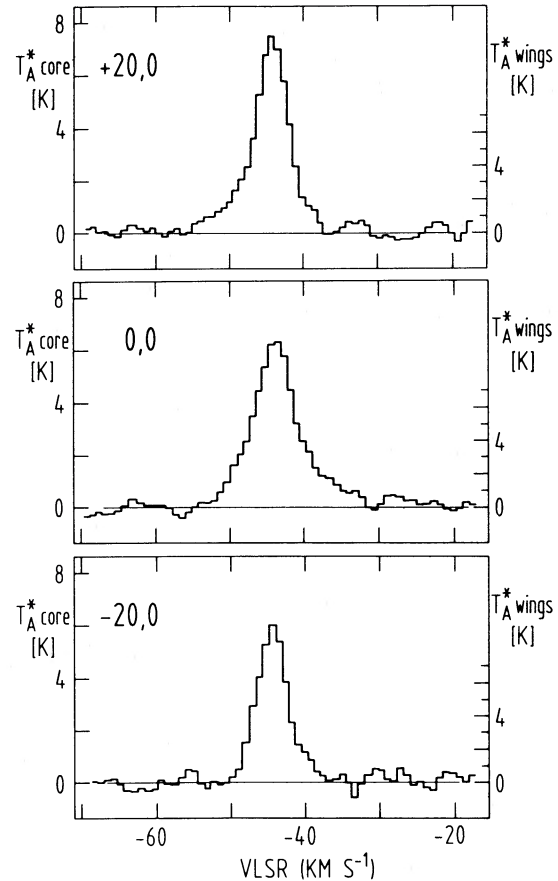


FIG. 1.—Three CO ($J = 3-2$) spectra of V645 Cyg at positions off the center as indicated (in arcsec) showing the variation of the line structure in the wings. Left-hand antenna temperature scale refers to the line core, right-hand scale to the line wings (different telescope efficiency for different source sizes as discussed in the text). Center: $\alpha = 21^{\text{h}}38^{\text{m}}10^{\text{s}}.6$, $\delta = +50^{\circ}00'43''$ (1950); integration time 20 minutes each spectrum [(0, 0): 50 minutes].

emission that exceeds $0.2 \text{ km s}^{-1} \text{ arcmin}^{-1}$. The distribution of integrated line intensity reveals a cloud slightly elongated in east-west direction; the peak in integrated intensity almost coincides with the position of N0 ($10''$ displacement).

The profiles also show prominent wings that extend over $\pm 15 \text{ km s}^{-1}$ in velocity. Figure 3 (Plate 9) shows the maps of wing emission integrated over the blue wing (-55.6 to -48.0 km s^{-1} , LSR) and over the red wing (-40.4 to -32.8 km s^{-1}), also superposed on the visible image. The centroid of the wing

TABLE 1
CO LINE CORE PARAMETERS

Transition	T_A^* (K)	V_{LSR} (km s^{-1})	ΔV (km s^{-1})	Beam	Reference
1-0.....	8.0 ± 0.5	$-44.3 \pm 1.$	<4.0	$60''$	1
	8.5 ± 0.5	-43.9 ± 0.7	<3.8	60	2
2-1.....	10.0 ± 1.5	$-44.0 \pm 1.$	4.4 ± 0.15	30	3
	8.7	-44.0 ± 0.7	5.0 ± 0.2	30	4
3-2.....	7.0 ± 0.7	$-44.3 \pm 1.$	5.1 ± 0.15	26	5

NOTE.—The antenna temperatures T_A^* are corrected for telescope efficiency and atmospheric losses.

REFERENCES.—(1) Bally and Lada 1983; (2) Rodríguez *et al.* 1981; (3) Margulis *et al.* 1988; (4) Torrelles *et al.* 1987; (5) this work.

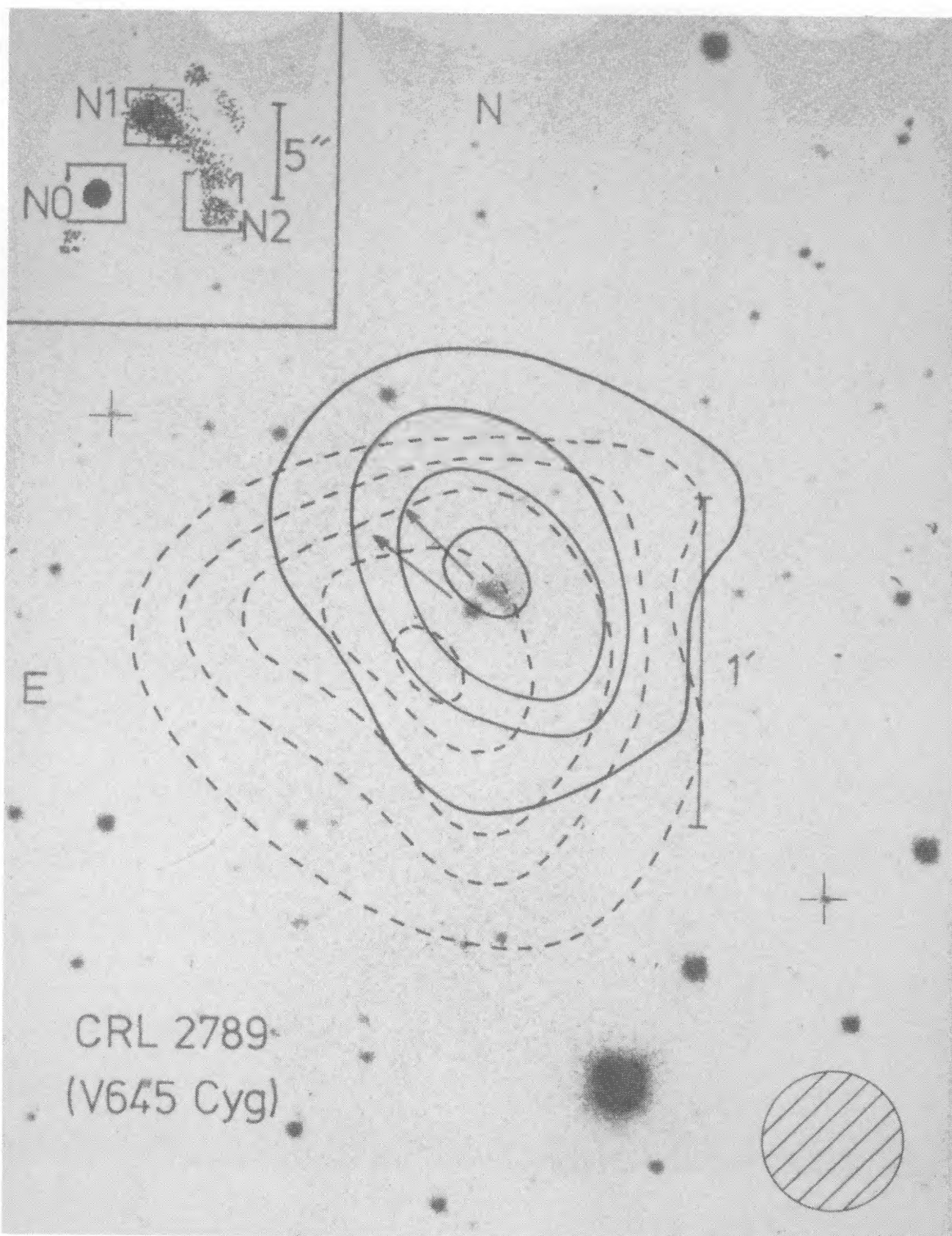


FIG. 2.—Contour map of integrated CO ($J = 3-2$) line intensity (lowest contour 19 K km s^{-1} , steps of 3 K km s^{-1}) in the velocity range of the line core (-48.0 to -40.4 km s^{-1}) superposed on the optical image given by Cohen (1977) (his Fig. 1) including the polarization vectors of N0 and N1 (values of about 13%). Beam size indicated; 0, 0 position: $\alpha = 21:38:10.0$, $\delta = +50:00:43$ (1950); crosses: grid of the CO map.

SCHULZ, BLACK *et al.* (see 341, 289)

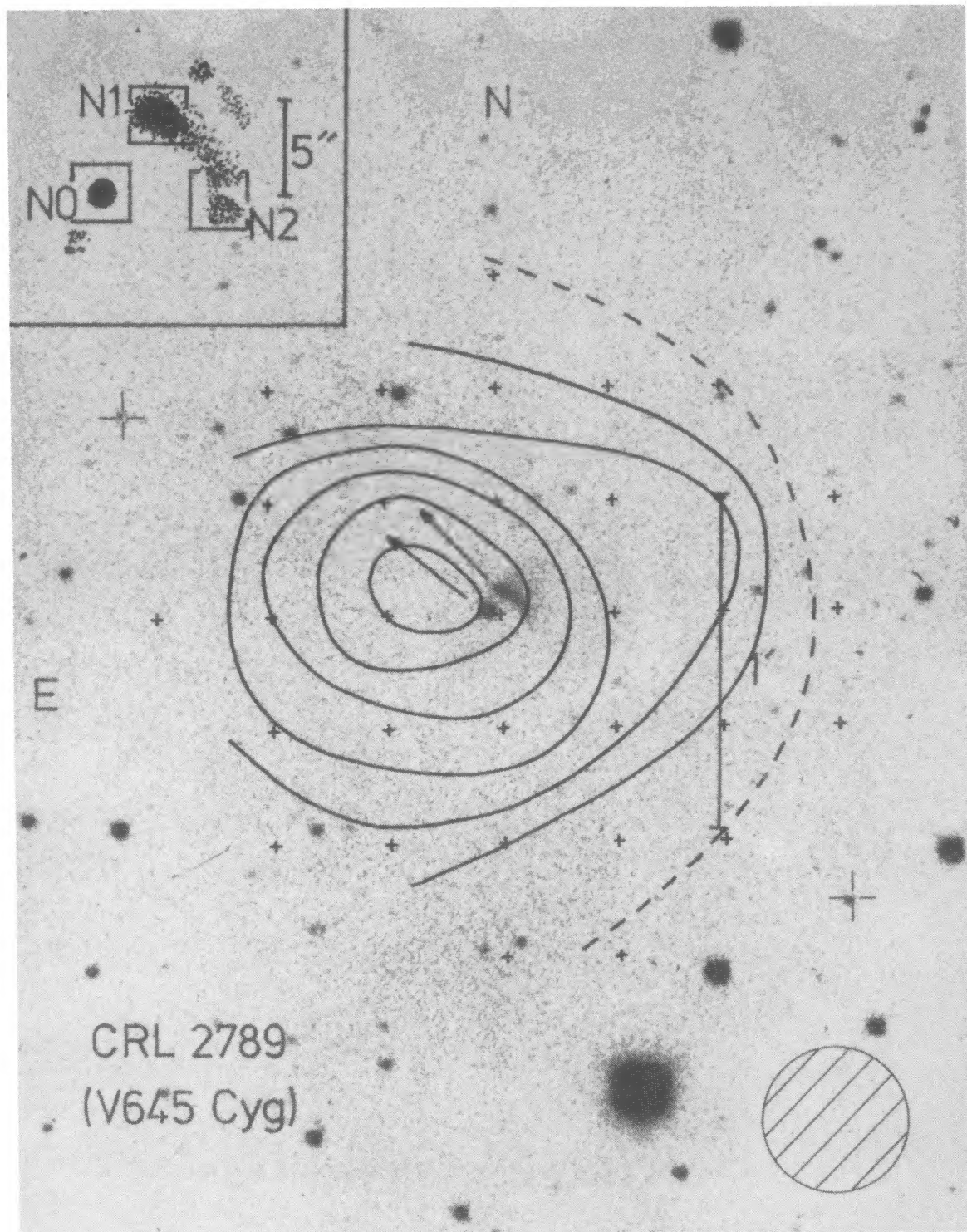


FIG. 3.—Contour map of integrated CO ($J = 3-2$) line wing emission [contours of 6, 9, 12, 15, (21, blue lobe only) K km s^{-1}] in the velocity ranges of -55.6 to -48.0 km s^{-1} (blue wing, *dashed lines*) and -40.0 to 32.8 km s^{-1} (red wing, *solid lines*) overlaid to the same image from Cohen (1977) as in Fig. 2. Beam size, grid, and center position as in Fig. 2.

SCHULZ, BLACK *et al.* (see 341, 289)

emission is centered on N0. Clearly, the areas of redshifted and blueshifted emission are displaced by $20''$ at a position angle of $-25^\circ \pm 20^\circ$. This displacement corresponds to a linear distance of $0.1D$ pc, where D is the distance to the source in kpc. The diameter of the half-power contour of each lobe is approximately $1'$ ($0.3D$ pc). From comparison with the previously published data, it is apparent that the ratio of wing intensity to core intensity is increasing with J' .

IV. DISCUSSION

The nature of V645 Cygni remains somewhat elusive. We summarize here those aspects of it that can be asserted with some confidence and discuss the implications of our characterization of the molecular outflow associated with it.

The visible spectrum of V645 Cyg, with its low-ionization emission lines, displaced absorption components, and P Cygni-type profiles, is characteristic of an Ae-type shell spectrum and indicates a fairly strong wind from the underlying star (Cohen 1977; Humphreys, Merrill, and Black 1980). There is no direct evidence for a very hot (i.e., O-type) photosphere, and the absence of appreciable microwave continuum emission shows that the underlying star does not currently support a well-developed photoionized nebula (Kwok 1981; Rodríguez, Torrelles, and Moran 1981; Rodríguez and Cantò 1983). There is a molecular cloud evidently associated with V645 Cyg, and indeed the bipolar outflow is clearly centered on the visible object N0 as discussed above. This provides strong, if circumstantial, evidence that V645 Cyg is a very young object. The infrared emission-line spectrum of V645 Cyg (Harvey and Lada 1980; McGregor, Persson, and Cohen 1984) also hints at the existence of a stellar wind and is similar to those of many other objects which are generally considered to be pre-main-sequence stars (Thompson 1982).

Goodrich (1986), comparing ($H-K$) and ($K-L$) colors, mentions that in the IR-two-color diagram, V645 Cyg is located in the regime of extreme Herbig-Ae/Be stars (i.e., far from normal Ae/Be stars). From the polarization measurements (Cohen 1977; Goodrich 1986; Lenzen 1986), it is inferred that the visible knot N0 is not identical with the central star. The visible objects must be regarded as reflection nebulae; according to very recent optical spectroscopy with high spatial resolution by Goodrich (1986) and Solf (1986), they contain small knots of line emission, at least one of them being typical for HH objects. The scattering geometry derived from the CCD image polarimetry of the filamentary nebulosities (Goodrich 1986; Lenzen 1986) indicates a location of the central source very close to N0; this is also suggested by the observations of H_2O maser emission (Lada *et al.* 1981). The appearance of the $10 \mu\text{m}$ silicate absorption feature in the spectrum of V645 Cyg implies that the central source is obscured in the line of sight towards the observer by at least 10 mag of visual extinction.

The published infrared photometry (Humphreys, Merrill, and Black 1980; Harvey and Wilking 1982) together with the fluxes from the *IRAS Point Source Catalog* show that V645 Cyg/AFGL 2789 has a considerable far-infrared excess. We find a total luminosity of $5000D^2$ (D in kpc) L_\odot from the integral of the published fluxes between 0.44 and $100 \mu\text{m}$. The infrared spectrum exhibits almost constant energy per decade between 4.8 and $100 \mu\text{m}$, and a non-negligible contribution to the total luminosity from the unobserved region longward of $100 \mu\text{m}$ cannot be excluded.

Derived properties of V645 related to its size and energetics all depend upon an uncertain distance. Given an accurate LSR radial velocity for the associated molecular cloud, it is tempting to assign a distance based upon standard models of galactic kinematics. The CO core velocity, $V_{\text{LSR}} = -44.5 \text{ km s}^{-1}$ at $l = 94.60$ and $b = -1.80$ would suggest distances of $D = 5.8$ and 6.3 kpc for the rotation curves of Gunn, Knapp, and Tremaine (1979) and Blitz (1979), respectively. It is well established—if often forgotten—that the interpretation of such radial velocities in this quadrant of the galaxy is severely hampered by the noncircular motions of the Perseus arm (e.g., Münch 1957; Rickard 1968; Humphreys 1976). For example, interstellar gas at $V_{\text{LSR}} > -50 \text{ km s}^{-1}$ in the direction $l = 115$ – 120 , for which the inferred kinematic distance lies in the range 4 – 6 kpc, is demonstrably no more than 1.7 – 2.5 kpc distant from the Sun (Black and Raymond 1984).

Chavarria *et al.* (1988) have photometrically determined the distances of many OB stars in H II regions within the second quadrant of our Galaxy ($l = 90$ – 180) and related them to their radial velocities. From their analysis, at $l = 94.6$ and $v_{\text{rad}} = -45 \text{ km s}^{-1}$ we would expect a distance of 3.0 ± 0.5 kpc for V645 Cyg. This is also in accordance with results of Spicker and Feitzinger (1986). The estimated visual extinction of $A_v \approx 4$ mag, about the same for all the nebulosities of V645 Cyg (Cohen 1977; Humphreys, Merrill, and Black 1980; McGregor, Persson, and Cohen 1984), is not inconsistent with a distance of 3 kpc according to the patterns of interstellar extinction in this direction (FitzGerald 1978; Neckel and Klare 1980), but a contribution to A_v from material associated with the source cannot be ruled out and makes this estimate of limited value. At this time, it seems safe to assert that a distance $D = 6$ kpc to V645 Cyg is an extreme upper limit; we adopt the more likely distance 3.0 ± 0.5 kpc hereafter.

The relatively quiescent cloud component of the CO line emission shows no velocity gradient larger than $0.2 \text{ km s}^{-1} \text{ arcmin}^{-1}$. The high-velocity line wings thus cannot be attributed to rotation of the cloud. The apparent increase in core line width with increasing J' is most simply explained by a corresponding increase in central optical depth for saturated lines. If the core emission is thermalized (i.e., if the excitation temperature T_{ex} is the same for all three observed transitions of CO), then an increasing optical depth with J , implies $T_{\text{ex}} > 20$ K. The lack of data on optically thin lines of isotopic varieties of CO precludes useful estimates of cloud mass and gas density and, considering also our still limited spatial resolution, makes a discussion of the cloud morphology as possible focussing agent of the bipolar flow premature.

The CO $J = 3$ – 2 line data reported here for the bipolar outflow allow the outflow to be described quantitatively as follows, the determined flow parameters being listed in Table 2. The observed line profiles can be separated approximately into cloud and outflow components by fitting Gaussian curves to the high-velocity wings. This suggests that the integrated intensity of the outflow emission is typically 1.5 times larger than that measured directly in the wings in the velocity intervals -55.6 to -48.0 and -40.4 to -32.8 km s^{-1} . At the central position of the outflow, we estimate an integrated intensity $\int T_b \Delta V = 190 \text{ K km s}^{-1}$ with a characteristic width of $\Delta V = 16 \text{ km s}^{-1}$, where ΔV is a lower limit because a broader pedestal may be hidden within the noise of our spectra and because of the possible inclination of the outflow direction. The brightness temperature T_b is obtained from the measured antenna temperature without assuming the Rayleigh-Jeans

TABLE 2
FLOW PARAMETERS

Parameter	Value
$\tau(J = 3-2)$	0.5
$N(\text{CO})$ (cm^{-2})	8×10^{16}
$\langle n(\text{H}_2) \rangle$ (cm^{-3})	$900 \left(\frac{\text{kpc}}{D} \right)$
$M(\text{H}_2)$ (M_\odot)	$1 \left(\frac{D}{\text{kpc}} \right)^2$
E_{kin} (ergs)	$2.7 \times 10^{45} \left(\frac{D}{\text{kpc}} \right)^2$
t (yr)	$2 \times 10^4 \left(\frac{D}{\text{kpc}} \right)$
L_{mech} (L_\odot)	$1 \left(\frac{D}{\text{kpc}} \right)$
$\langle \dot{M}v \rangle$ ($M_\odot \text{ yr}^{-1} \text{ km s}^{-1}$)	$8 \times 10^{-4} \left(\frac{D}{\text{kpc}} \right)$
$\langle \dot{M}v(\text{wind}) \rangle$ ($M_\odot \text{ yr}^{-1} \text{ km s}^{-1}$)	1.7×10^{-3}
L_{tot} (L_\odot)	$5000 \left(\frac{D}{\text{kpc}} \right)^2$
Adopted $T_k = T$ (K)	30

approximation and includes also the correction for the complicated beam response to a small extended source as discussed in § II. If we assume that we have correctly subtracted the emission of the ambient cloud so that the only remaining background is the 2.7 K cosmic background radiation and if we further assume that the CO is thermalized at a temperature T_{ex} , then the adopted brightness temperature and line width imply an optical depth $\tau < 0.6$ in the $J = 3-2$ line and a CO column density $N(\text{CO}) \approx 8 \times 10^{16} \text{ cm}^{-2}$ for any value of $20 < T_{\text{ex}} < 100 \text{ K}$. The low τ is in accordance with the fact that the strength of the wings is increasing with J' . If the outflow emitting region is taken to be a cube 1' on each side and if the CO abundance is taken to be $n(\text{H}_2)/n(\text{CO}) = 10^4$, then the mean density is $n(\text{H}_2) = 900D^{-1} \text{ cm}^{-3}$, and the total mass is $M = 1.0D^2$ solar masses. If the volume density is indeed less than 1000 cm^{-3} , then the assumption of thermalized emission may be invalid, in which case the inferred mass becomes a lower limit; if, on the other hand, the outflow gas is clumped, the local density exceeds the mean and the derived parameters should represent useful estimates. For a characteristic flow velocity of 16 km s^{-1} , the implied kinetic energy in the flow is of the order of $3 \times 10^{45}D^2$ ergs. If this flow has been steady over its entire lifetime of 2×10^4D yr, then the mean mechanical luminosity of the outflow is of the order of $L_{\text{mech}} = 1D L_\odot$. The noise of our spectra does not allow us to investigate deceleration (the size of the flow as a function of velocity). The inferred luminosity of the outflow is both small in absolute terms and small in relation to the bolometric luminosity of the underlying star, $L_{\text{mech}}/L_* = 0.00016D^{-1}$ (Lada 1985); the corresponding momentum transfer rate $\dot{M}v = 8 \times 10^{-4}D M_\odot \text{ yr}^{-1} \text{ km s}^{-1}$. The upper limit on the stellar mass loss rate quoted by Kwok (1981) and the apparent expansion velocity of the circumstellar shell, 330 km s^{-1} , of Humphreys, Merrill, and Black (1980) suggest that the central star may be energetically capable of driving the bipolar outflow by its ionized stellar wind. In this case, we would not be faced with the momentum problem often met in outflow sources revealing a large discrepancy

between observed stellar wind and molecular outflow momentum.

While this paper was in preparation, Torrelles *et al.* (1987) published observations of V645 Cyg in the CO $J = 2-1$ line at 30" resolution which confirm a bipolar outflow structure—although not as clearly as the $J = 3-2$ measurements presented here. Torrelles *et al.* have adopted a distance of 6 kpc without comment or justification which would yield overestimates of all distant-dependent parameters of the object.

The available data still do not permit a final model of V645 Cyg. On the one hand, a preferential projected axis for the entire object is defined by the outflow. The large discrepancy between low visual extinction of the nebulae and high visual extinction in front of the central source hints at a very anisotropic dust distribution, and one may be tempted to infer the presence of a disk. But on the other hand, the puzzling variety of features of reflected light, shock-ionized nebula emission (Goodrich 1986; Solf 1986), and P Cyg absorption with different velocities ranging from almost rest velocity to -600 km s^{-1} leave us still in some confusion about the true geometry of the object. In particular, the fact that the blueshifted visual emission is located on the side of the redshifted CO gas while we do not see any redshifted visual/near-infrared emission at all, still needs an explanation. At this point, the suggestion of a shape similar to that of an hourglass—possibly warped—for the entire object, seen almost “from its top,” with a very inhomogeneous clumpy distribution of matter located on the near side of a molecular cloud could provide a first hypothesis.

V. CONCLUSIONS

From our analysis of a CO ($J = 3-2$) line map at 26" angular resolution in the molecular cloud in the direction of V645 Cyg together with pertinent results from the literature, we conclude the following:

1. The kinematic distance of 6 kpc from standard models of galactic kinematics is almost certainly invalid. From a comparison of several analyses we obtain 3 ± 0.5 kpc as a more likely value.

2. The total luminosity of V645 Cyg/AFGL 2789 is $5000 (D/\text{kpc})^2 L_\odot$, i.e., of the order of $5 \times 10^4 L_\odot$ for an adopted distance of 3 kpc.

3. The bulk of molecular gas observed in CO is contained in a quiescent cloud at low temperature with V645 Cyg being located at the near side of this cloud.

4. The observed line wings reflect outflowing gas which is optically thin in CO (3-2); the outflow is cold, of low velocity and low mass, and is quite old. The momentum transferred by the ionized stellar wind seems to be sufficient to drive the molecular outflow.

5. The outflow is bipolar but weakly collimated—favoring a more face-on rather than an edge-on view toward the object—with its axis about perpendicular to the vector of optical polarization of the central knot N0. The complicated spatial geometry of the object cannot be unequivocally clarified and may be fully understood only with the help of observations of still higher spatial resolution.

We are grateful to P. A. Strittmatter, P. G. Mezger, and F. H. Chaffee for support and encouragement. The technical staff of the Multiple Mirror Telescope Observatory provided excellent support for this project with its unusual operational demands. K. Ruf of the Max-Planck-Institut für Radioastronomie is thanked for logistical assistance. We have benefited

from discussions with M. Margulis, C. M. Walmsley, R. Güsten, C. Henkel, and T. L. Wilson. Research on star-forming

regions at the University of Arizona is supported in part by NASA through grant NAGW-763.

REFERENCES

- Bally, J., and Lada, C. J. 1983, *Ap. J.*, **265**, 824.
 Black, J. H., and Raymond, J. C. 1984, *A.J.*, **89**, 411.
 Blitz, L. 1979, *Ap. J. (Letters)*, **231**, L115.
 Chavarría, K. C., Hasse, I., Moreno, M. A., and Pismis, P. 1988, in preparation.
 Cohen, M. 1977, *Ap. J.*, **215**, 533.
 FitzGerald, M. P. 1968, *A.J.*, **73**, 983.
 Goodrich, R. V. 1986, *Ap. J.*, **311**, 882.
 Gunn, J. E., Knapp, G. R., and Tremaine, S. 1979, *A.J.*, **84**, 1181.
 Harvey, P. M., and Lada, C. J. 1980, *Ap. J.*, **237**, 61.
 Harvey, P. M., and Wilking, B. A. 1982, *Pub. A.S.P.*, **94**, 285.
 Hoffmeister, C., Rohlf, E., and Ahnert, P. 1951, *Veröff. Sternw. Sonneberg*, Vol. **1**, No. 5.
 Humphreys, R. M. 1976, *Ap. J.*, **206**, 114.
 Humphreys, R. M., Merrill, K. M., and Black, J. H. 1980, *Ap. J. (Letters)*, **237**, L17.
IRAS Point Source Catalog. 1984, Joint IRAS Science Working Group (Washington: US Government Printing Office).
 Joyce, R. R., Capps, R. W., Gillett, F. C., Grasdalen, G., Kleinmann, S. G., and Sargent, D. G. 1977, *Ap. J. (Letters)*, **213**, L125.
 Kwok, S. 1981, *Pub. A.S.P.*, **93**, 361.
 Lada, C. L. 1985, *Ann. Rev. Astr. Ap.*, **23**, 267.
 Lada, C. J., Blitz, L., Reid, M. J., and Moran, J. M. 1981, *Ap. J.*, **243**, 769.
 Lenzen, R. 1986, *Astr. Ap.*, **173**, 124.
 Margulis, M., Lada, C. J., Thronson, H. A., and Wolf, G. 1988, in preparation.
 McGregor, P. J., Persson, S. E., and Cohen, J. G. 1984, *Ap. J.*, **286**, 609.
 Morris, M., and Kazes, I. 1982, *Astr. Ap.*, **111**, 239.
 Münch, G. 1957, *Ap. J.*, **125**, 42.
 Neckel, Th., and Klare, G. 1980, *Astr. Ap. Suppl.*, **42**, 251.
 Price, S. D., and Walker, R. G. 1976, US Air Force Geophysical Laboratory Report AFGL-TR-76-0208.
 Rickard, J. J. 1968, *Ap. J.*, **152**, 1019.
 Rodríguez, L. F., and Cantò, J. 1983, *Rev. Mexicana Astr. Ap.*, **8**, 163.
 Rodríguez, L. F., Torrelles, J. M., and Moran, J. M. 1981, *A.J.*, **86**, 1245.
 Spicker, J., and Feitzinger, J. V. 1986, *Astr. Ap.*, **163**, 43.
 Solf, J. 1986, private communication.
 Thompson, R. I. 1982, *Ap. J.*, **257**, 171.
 Torrelles, J. M., Anglada, G., Rodríguez, L. F., Cantò, J., and Barral, J. F. 1987, *Astr. Ap.*, **177**, 171.

JOHN H. BLACK, CHARLES J. LADA, ROBERT N. MARTIN, and BOBBY L. ULICH: Steward Observatory, University of Arizona, Tucson, AZ 85721

RONALD L. SNELL and NEIL J. ERICKSON: Five College Radio Astronomy Observatory, 619 Lederle Graduate Research Center, University of Massachusetts, Amherst, MA 01003

ANDREAS SCHULZ: Max-Planck-Institut für Radioastronomie, Auf dem Huegel 69, 5300 Bonn 1, Federal Republic of Germany